The Original

DEEP LEARNING MODEL WITH HYBRID CHAOTIC SAND CAT SWARM OPTIMIZATION AND SAILFISH OPTIMIZER FOR ARRHYTHMIA ECG SIGNAL CLASSIFICATION

Pushp Raj Tripathi[1], Dr Rakesh Kumar Saxena[2]

[1]Research scholar, Poornima University Jaipur, Orcid Id- 0009-0006-2535-785X , Email:- mtechpushp@gmail.com
[2]Professor Poornima University Jaipur, Orcid Id- 0000-0002-6453-6053, Email:- saxenark06@gmail.com

ABSTRACT
Arrhythmia of the heart is a collection of erratic heartbeats that result from an anomaly with the coronary electrical structure. The electrocardiogram or ECG measurements can detect cardiovascular rhythmic abnormalities, known as arrhythmias. On the other hand, seeking experts to assess an enormous amount of ECG data consumes an undue amount of medical infrastructure. Deep learning, also known as DL, maybe the better choice for fast and automatic categorization with proper training. The current study presents an innovative hybrid optimizer for the feature selection process in arrhythmias of the heart. The noisy signal of ECG extracted from the dataset of MIT-BIH Arrhythmia was pre-processed by the utilization of finite impulsive response (FIR) and Infinite impulsive response (IIR) to remove the noises of technical as well as biological, leading to misclassification of arrhythmia. The pre-processed wave has redundant features which are removed with the acquisition of the proposed hybrid model optimizer of Chaotic sand cat swarm optimizer with sailfish optimizer. The non-redundant features accumulated from the proposed model are employed under the classifier of the Interpretable Temporal Attention Network (ITA Net). It is further classified into five classes supraventricular ectopic (S), non-ectopic (N), fusion (F), ventricular ectopic (V), and unknown (Q). We can confirm that the proposed approach encouragingly outperforms the current arrhythmia categorization.

KEYWORDS: arrhythmia, ECG, Feature selection, Chaotic Sand Cat Swarm Optimization algorithm, Sailfish Optimizer.

1. INTRODUCTION

Cardiovascular illnesses are the most common cause relating to human death, killing about 17 million people each year. A prevalent medical condition that seriously compromises the wellness of people, especially middle-income along with older persons, is heart disease [1]. In contrast to the World Heart Federation of Australia, middle-class as well as financially less fortunate individuals account for a third of all CVD fatalities.

The cardiovascular system must circulate oxygenated blood throughout the human body and remove impure blood containing carbon dioxide and other toxins [2]. The Sino atrial node is a natural pacemaker located in the coronary arteries' right atrium, which generates an electrical impulse. It creates an impulse that activates the cardiovascular system's pumping machinery. The early detection of arrhythmias of the heart saves lives [3]. The greatest technique to identify cardiac arrhythmias is an electrical cardiogram signal. The ECG constitutes an apparent series of incidents that gauges the cardiac electrical conduction in the present instant [4].

Any variations in cardiac rhythm abnormalities or ECG abnormalities indicate underlying cardiovascular disorders such as arrhythmia. Electrode put on the skin may be utilized for collecting a heart rhythm via ECG signal, which relies on the typical 12-lead ECG that monitors the potential electricity from 10 electrodes dispersed throughout the body's surface [5]. Any doctor will find it challenging and time-intensive to continually analyze an ECG signal like this one. Computer-assisted diagnostic methods are widely utilized to analyze ECG information and recognize arrhythmias due to high reliability and precision [6]. As a result, it is crucial to monitor the signals of ECG for early detection of disorders such as arrhythmias.

Many methods involving machine learning have been developed in the scientific community to detect arrhythmia utilizing data from ECG [7]. Traditional artificial intelligence approaches cannot be applied unless first implementing a feature-extracting strategy. Before using characteristic ML algorithms, a feature extraction procedure is necessary, which removes numerous handmade elements that influence classification outcomes [8]. However, because robotic extraction of attributes does not leverage the fundamental data stored in the database, it is expensive as well as time-consuming. An increasingly prevalent problem in ML-based classification systems is overfitting from occurring [9].

A DL methodology is most appropriate for the challenge since it has several distinct layers of neurons in a network of neurons and can find a way to identify the ECG signal in a shorter time with reliable results [10]. These results allowed them to break down each into various distinct beats to extract data on all types of arrhythmia signals. Stated differently, the integration of DL into the classification of arrhythmias is still an emerging discipline. Further study is needed to develop an effective smart system that might replace clinicians in the future and assist in identifying cardiac illnesses.

Despite being assigned as the signature methodology for the categorization of cardiac arrhythmia deep machine learning has significant shortcomings over the existing research which are discussed below in sections of related studies.
To address the drawbacks of previous research, we recommended a model based on DL with a hybrid model of a chaotic sand cat optimizing algorithm and a sail fish optimization to improve the selection of features process, which can influence the identification of arrhythmia.

This article contributes,

- The ECG extracted from the dataset of MIT-BIH Arrhythmia was processed with IIR and FIR noise filters to remove technical and biological noise during ECG diagnosis.
- The noise-removed pre-processed image was put through to the presented hybrid optimization approach of the CSCSO with SO to remove redundant characteristics for arrhythmias categorization.
- The proposed hybrid algorithm's not redundant characteristics have been divided into five categories by utilizing the Interpretable Temporal Attention Network (ITA Net) classifier: supraventricular ectopic (S), non-ectopic (N), fusion (F), ventricular ectopic (V), and unknown (Q).

The proposed study is divided into five components, the first of which introduces a classification of arrhythmias from ECG data. Section 2 provides an overall review of the currently conducted research on arrhythmia categorization. Section 3 provides a comprehensive overview of both the preliminary and suggested methodologies. Section 4. Illustrates the findings of the article. Section 5 closes the article as well as discusses the scope of future projects.

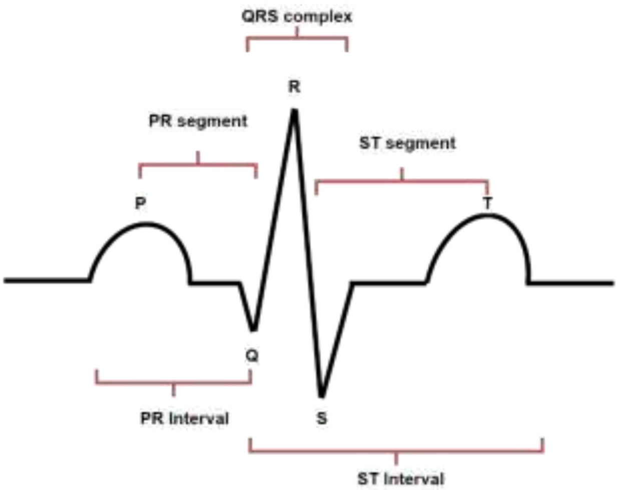

Figure 1. Illustrates ECG of the heart.

2. RELATED WORKS:

Pooja Sharma et al. [11] devised a hybrid approach to classify arrhythmias through cardiovascular irregularity. The CS+DWT+SVM-FFBPNN algorithm classifies signals into five distinct groups by merging SVM and FFBPNN. ECG readings from the MIT-BIH dataset have been divided using the Cuckoo search technique. The present research uses the Discrete wavelet transformation approach in the preliminary processing phase to reduce fundamental noise while enhancing classification accuracy. The cuckoo search method is used to improve the method for choosing features. The computational cost of integrating the cuckoo search algorithm using neural networks may provide issues in applications that operate in real-time.
Ahmet C¸ınara and Seda Arslan Tuncerb [12] established a network using DL that uses a combination of classifier models to classify ECG signals into the congestive cardiac disease of arrhythmia normal sinus, and heart failure. The Alexnet-CNN combination was created by combining Alexnet classifiers with the Support vector machine technique and substituting the softmax layers that appear right before the final pooling layer with neural networks. The fact that the present research did not address the issue underlying noise in the ECG data, which could have affected categorization, is regarded as a severe shortcoming.

To improve the precision of diagnosing cardiovascular abnormalities, Atta-ur Rahman et al. [13] established the CAA-TL training model to classify arrhythmias from ECG signals utilizing ResNet50, AlexNet, and SqueezeNet using DL methods. During the investigation, the MIT-BIH database was evaluated and the information was extracted from the Kaggle platform. It compares various DL algorithms and gains significant insights into their effectiveness in arrhythmias identification works. One of the significant drawbacks that emerged during the research process is the need for time.

Fakheraldin Y. O. Abdalla et al. [14] established an 11-layer deeply convolution framework to categorize arrhythmias. This 11-layer-by-layer structure model consists of four layers with convolution that are swapped with four max pooling layers and three satisfactorily linked layers. They analyzed the MIT-BIH database, which is extracted from Physionet, to ensure that the data was appropriate. The understanding of the outcome stems from making decision categorization due to the lack of a different classifier.

Adel A. Ahmed et al. [15] introduced the 1-D deep convoluted model for cardiovascular arrhythmia classification to overcome the limitations of standard ECGs throughout assessment. To ensure the effective collection of the P-wave, T-wave, and QRS Complex components, this model separates the electrical signal concentrated on the R-peak location. This paper failed to examine the influence of noise on ECG performance, which has a significant impact throughout the immediate execution process.

By altering the SCA, Pooja Sharma et al. [16] developed LA-SCA. The Wilcoxon rank-sum test, which depends on the number of generations before them is employed to examine the developed LA-SCA model. An OBL model is subsequently implemented to find the best solution. This work uses discrete wavelet processing to categorize ECG data and extract the QRS complex characteristics. However, irregular ECG waves are examined using the Fourier transformation, which results in informational degradation.

Amin Ullah et al. [17] developed a 2D CNN with eight layers to classify the heartbeat based on ECG signals obtained from MIT-BIH datasets. They employed a Fourier transform of a short time to extract the well defined attributes from the 1-D ECG signals, resulting in the spectrogram of 2-D in nature. The layer consists of four convolutional layers that combine information as well as four layers of pooling that extract characteristics from the spectroscopy input.

Mengze Wu et al. [18] created a twelve-layer deep convoluted neural network to classify ECG information from a heartbeat into five categories. The study uses a variety of filters, including bandpass, low-pass, and wavelet changes, to remove noise from the ECG data. Ten distinct verifications by cross-valid algorithms are employed across the research process to improve the durability along with the efficacy of the predictive framework. The research project did not use any sort of optimization techniques, which could have influenced the enhancement of the research's produced models.

Surbhi Bhatia et al. [19] developed a combination model of a CNN with a bidirectional LSTM network. The MIT-BIH database was reviewed during the investigation. To address the disparity issue, the dataset was overestimated using the strategy of SMOTE. The SMOTE was utilized to resolve disparities in classes and failed to tackle excessive fitting or oversampling.

Parul Madan et al. [20] established a hybrid DL-based technique for the automatic identification of arrhythmias. The model that was created combines complicated and LSTM networks. 1D images of ECG were converted into 2D images of scalograms to enable noisy filtering, resulting in an improved assessment technique.

According to the above-mentioned most recent publications, the investigation's key flaw is non-noise removal, since much previous research occurs without noise removal, which has a possible effect on the identification of arrhythmias from ECG signals. In addition, existing research raises the computational challenge and time spent on the mathematical framework. Finally, due to limitations in machine learning approaches, DL provides a well-suited approach for arrhythmia identification. However, the primary limitation in the study area is the lack of a classifier as a feature selection method, which has a significant impact on the misdiagnosis of Arrhythmia disease. Our research paper has been organized in such a way that it addresses the difficulties mentioned above.

3. METHODOLOGY

3.1. Dataset acquistion

In this work, the BIH Arrhythmia Laboratory got the MIT-BIH arrhythmia database. It contains 23 records selected at randomness from this set, as well as 25 records chosen from the same set, all of which have a rate of sampling of 360 Hz and are roughly 30 minutes long [21]. It has several heartbeat types, with five of them containing meaningful samples denoted as N, S, V, F, and Q, numbered 0, 1, 2, 3, and 4, accordingly. The AAMI classes were used as shown in Table 1 below, dividing fifteen different types of ECG signals into five categories: S (supraventricular ectopic beats), N (non-ectopic beats), F (fusion beats), V (ventricular ectopic beats), and Q (unknown beats). To validate the study's proposed approach, signals that had been extracted from the database were transformed into waves. Figure 2 illustrates the general intellectual structure of the research.

Table 1. Depicts the class of the MIT-BIH arrhythmia dataset

AAMI CLASS	TYPES OF HEARTBEAT	NUMBERS
Supraventricular ectopic	S	2
Non-ectopic	N	75028
Fusion	F	802
Ventricular ectopic	V	7129
Unknown	Q	33

3.2. Pre-processing

The existence of numerous physiological disturbances, as well as technological noises such as electrical lines, communication line interferences, and electrode movement degrades the overall quality of the ECG signal. Because of the low amplitude, the electrical signal is corrupted, resulting in an incorrect diagnosis during processing [22]. The suggested technique eliminates noise in an ECG signal by utilizing both finite and infinite impulse responses.

3.2.1. FIR

FIR filters are distinguished by phase linearity, which allows the final signal to have zero abnormal time displacement between its components. This property enables the myocardium complex's sine rhythms to maintain a division as time passes throughout the electronic processing of the ECG.

The transfer function for the FIR filter is

$$H(z) = \sum_{k=0}^{N-1} h(k)z^{-k} \quad (1)$$

Where, h(k) with k = 0, 1... N−1, are the coefficients of the filter impulse response, Hz is the filter transfer function and N is the order of the filter.

The mathematical model of the FIR function is

$$y(z) = \int_0^T x(t-z)h(z)dz \quad (2)$$

Where the output function is denoted as yz and the input is x(z). The convolution of the input with a transfer function h(z) provides a filtered output yz.

3.2.2. IIR

However, the IIR filtering has an irregular phase response, implying a changing grouping latency and distortion in the signal over time that does not appear in its frequency spectrum. This sort of filter decreases the shifting of the ECG's baseline by producing absorption and deformation in the audio frequency spectrum. It is characterized by a recursive equation in which h[k] is the filter impulsive response that has an infinite value, bk and ak are co-efficient of the filter while x[n] and y[n] are input and output filters.

$$y[n] = \sum_{k=0}^{\infty} h[k]x[n-k] = \sum_{k=0}^{N} b_k x[n-k] - \sum_{k=1}^{M} a_k y[n-k] \quad (3)$$

In the Z domain, the IIR filter transfer function is represented as

$$H(z) = \frac{\sum_{k=0}^{N} b_k z^{-k}}{1+\sum_{k=1}^{M} a_k z^{-k}} \quad (4)$$

All technical and biological sounds encoded in the ECG signals have been eliminated after using filters such as FIR as well as IIR.

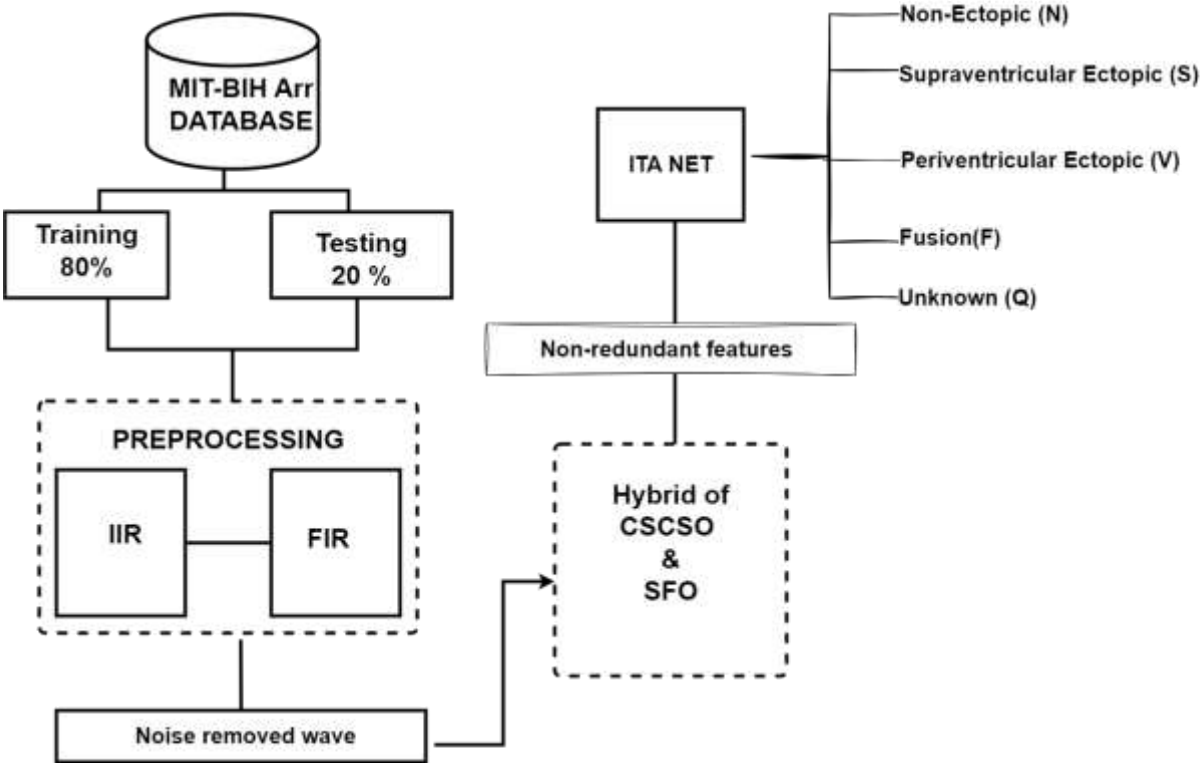

Figure 2. Illustrates the conceptual framework of the study

3.3. Feature selection

The pre-processed waves were fed into the feature selection technique, which reduces the space of redundant features. In the geometrical progress of computing technology, proper identification of arrhythmias cardiac conditions is critical due to difficulties with overfitting and computational effectiveness [23]. To address this issue, our study team created a hybrid optimization model that combines the CSCSO algorithm alongside the SO algorithm.

3.3.1. CSCSO Algorithm

In mathematics, the fundamental deterministic kinetic structure's innate randomness is referred regarded as chaos, and erratic structures can be thought of as the causes of randomized. The chaos-based optimization technique translates surprising patterns using chaotic map data to create design factors as part of the whole process of manipulation. The CSCSO technique provides two different approaches for phased position updates. One is the regular position updating technique, while another is based on the chaos model. Each of them has an equal likelihood of achieving an appropriate weight.

Every cat assigned as a search agent is designed as a vector and the duration is issue approached on the direct vision. The efficacy of the algorithm is measured using the fitness value of each task (eq. 5).

$$Fitness = f(Sand\ Cat) = f(SC_1, SC_2, \ldots, SC_n); \forall x_i(is\ calculated\ for\ t\ time) \quad (5)$$

The mathematical models that are effective in seeking are considered as the exploration phase and exploitation phase of the SCSO is given below.

$$\vec{X}(t+1) = \begin{cases} \overrightarrow{X_b}(t) - \vec{X}_{rnd}.\cos(\theta).\vec{r} & |R| \leq 1; exploitation(a) \\ \vec{r}.\left(\overrightarrow{X_c}(t) - rand.\overrightarrow{X_k}(t)\right) & |R| > 1; exploration(b) \end{cases} \quad (6)$$

Where t represents the current iteration, and T indicates the maximum number of iterations. In general, the behavior model of the SCSO algorithm in updating the location is presented in Equation (7), both in the exploitation phase and in the exploration phase:

$$\vec{X}\ (t+1) = \begin{cases} if\ p < 0.5 \equiv Eq.5 \\ if\ p \geq 0.5\ \equiv Eq.10 \end{cases} \quad (7)$$

Where p is a randomized integer between 0 and 1. The C parameter is the most essential variable in completing a task. The value of this parameter directly influences the R factor. The C parameter enhances the CSCSO algorithm's versatility by playing a one-to-one role during its exploration and extraction. As a result, parameter C has been established for use in the Chaotic Sand Cat Swarm Optimisation algorithm, which is symbolized by Equations (9). C additionally has a crucial part in demonstrating fair and equitable behavior during exploration and exploitation. This refers to the usability of the exploration along with the exploration phases.

$$S = 2^k; k \geq 1 \quad (8)$$

$$C = s - s\left(\frac{\sqrt[T]{e^t} - 1}{e - 1}\right) \quad (9)$$

Where K represents the constant factor. This parameter (K) influences the amount of weight the algorithm assigns for each stage. The exploring phase has a greater likelihood with this equation. Focusing greater attention on the investigation phase of the CSCSO algorithm produces favorable outcomes in confined issues. This new equation also has implications for both parameters R and r. Since the R parameter is reliant on C, its changing span is exactly lowered. R is a random value in vary of [-2C, 2C]. While R turns into less compared to or equal to a single one, the CSCSO methods require agents to seem to exploit; as an alternative, search employees must examine and discover prey. This is used whenever the p-value is less than 0.5. The chaotic maps are assigned as a substitute. Early convergence as well as local optimal entrapment can be prevented in this way. Equations (10) and (11) are used to compute the parameters of R and r that are anticipated to be generated as a result of the chaotic map's impact.

$$\vec{R} = 2 \times \vec{c} \times\ m - \vec{c} \quad (10)$$

$$\vec{r} = \vec{c} \times m \quad (11)$$

$$\vec{X}(t+1) = \begin{cases} \overrightarrow{X_b}(t) - \overrightarrow{X_{rnd}}.\cos\theta.\vec{r} & |R| \leq 1(a) \\ \vec{r}.\left(\overrightarrow{X_c}(t) - m.\overrightarrow{X_t}(t)\right) & |R| > 1(b) \end{cases} \quad (12)$$

A chaotic map is employed to compute the chaotic vector m. Equation (12), outlined above, is implemented to generate an overall conceptual representation of the CSCSO. Owing to the results of the recommended approach, it will find more potential localized territories in global spaces with a precise and rapid resolution rate across a range of scenarios, especially restricted issue areas for optimization.

3.3.2. Sailfish Optimizer

SOA is based on a population meta-heuristic technique based on the attack-alternation strategy of a school of sardines. The program aims to randomly allocate the movements of all the agents of search (sailfish and sardine) as much as feasible. Sailfishes are spread throughout the area of search, whereas sardines help to find the perfect solution.

The method selects the sardines with the highest fitness score as the 'damaged' fish, represented as (Psrdinji) at ithiteration. Sardines along with sailfish placements are updated with every repetition. In each iteration, the relative position of a sailfish is modified using the 'elite' sailfish PSlfbestiand the 'damaged' sardine according to a certain criterion. The location of sailfish along with sardines is adjusted at every iteration, denoted by i+. The (elite) and (injured) alter as well as update the location of a sailfish to an alternate position denoted as PSlf_newi+1 and formulated as

$$P^{i+1}_{Slf\_new} = P^{i}_{Slfbest}\text{-}\lambda\text{i}\left(rand * \frac{P^{i}_{Slfbest} + P^{i}_{srdinj}}{2} - P^{i}_{Slf\_old}\right) \quad (13)$$

PSlf_oldi Represents the sailfish's (Slf) prior coordinates, while rnd specifies a random sum between 0 and 1. Equation (14) generates the coefficient λi.

$$\lambda i = (2 * rand(0,1) * PrD - PrD) \quad (14)$$

The prey density (PrD) drops with each cycle of group hunting because the number of prey decreases.

$$PrD = 1 - \frac{No._{Slf}}{No._{Slf} - No._{Srd}} \quad (15)$$

Sailfish along with sardine numbers are denoted as No.Slf andNo.Srd, respectively. The total number of sailfish (No.Slf) can be determined by applying Eq. (16):

$$No._{Slf} = No._{Srd} * \% \quad (16)$$

The sardine number is always considered to be larger than the sailfish population at the start. In every successive iteration, the sardine locations are updated following Eq. (17).

$$P_{Srd\_new}^{i+1} = rand * \left(P_{Slfbest}^{i} - P_{Srd_{old}}^{i} + ATP\right) \quad (17)$$

PSrd_newi+1 as well as PSrd_oldirepresent the updated along with previous locations of sardines, accordingly. The ATP indicates the strength of the sailfish attack at every i th iteration and it may be determined via Eq. (18):

$$ATP = A * \left(1 - (2 * Itr * \lambda)\right) \quad (18)$$

A decrease in ATP may aid in search activity concentration. Eqs. (19) and (20) are used to calculate the number of variables present in the sardines and the amount of sardines that modify their positions based on their ATP parameter.

$$\gamma = ATP * No._{Srd} \quad (19)$$

$$\delta = ATP * \mu \quad (20)$$

Where µ and No.Srd Stands for the total number of parameters and the sardine quantity, respectively. Sardines may evade the most ferocious sailfish since their attack strength diminishes with every iteration. The ideal balance between the two of them is determined using the ATP variable. This aids in striking an equilibrium between space and its extraction and exploration.

3.3.3. The proposed hybrid model of Chaotic Sand Cat Swarm Optimization Algorithm and Sailfish Optimizer.

By harmonizing the search area and concentrating on the best solutions among them, the chaotic sand cat swarm optimization method and the sailing fish optimizer improve both the phase of exploration and extraction phases. The chaotic maps of the CSCSO optimizing algorithm help to improve the deception of local optima since they can accurately evaluate every inch of the search space. Better outcomes can be obtained by a sailfish optimization with a high convergence rate.

3.3.3.1. Initialization phase

Let N represent the population size in the Dimensionality D search region. Use the chaotic map to set the position in the exploring region by the CSCSO optimizer's protocol. Let Pio represent the ithsand cat's starting position. Analyze the sand cats' fitness, which is represented as:

$$Fit(X_i^0) = f(X_i^0), \forall\, i \in \{1,2,\dots,N\} \quad (21)$$

3.3.3.2. Exploration phase: CSCSO

Following the phase of initialization, the procedure for optimization developed during the different iterations. Every iteration's position (Xit+1) is modified. The direction and the quantity of the beginning velocity of the sand cat are taken into account in the newly created position vector.

The updated position can be computed as

$$X_i^{t+1} = X_i^t + V_i^t \quad (22)$$

Both the modified position's fitness and application of erratic maps are being considered. It can be expressed as

$$Fitness(\, X_i^{t+1}) = f(X_i^{t+1}) = f(X_i^t + V_i^t) \quad (23)$$

Generally speaking, Equation (22), during the exploitation and exploration phases, presents a mathematical model of the CSCSO algorithms in location updating. Next, assess and revise the search space's potential localized (Pit+1) and worldwide optimum (Gt+1).

$$P_i^{t+1} = \begin{cases} X_i^{t+1} \; if \; f(X_i^{t+1}) > f(P_i^t) \\ P_i^t \qquad otherwise \end{cases} \quad (24)$$

$$G^{t+1} = \begin{cases} X_i^{t+1} \; if \; f(X_i^{t+1}) > f(G^t) \\ G^t \qquad otherwise \end{cases} \quad (25)$$

Assess if the standards for convergence were satisfied after the allotted number of repetitions, assess fitness, or evaluate if there has been no apparent improvement over the repetition before entering the CSCSO phase.

3.3.3.3. Hybridizing Point

The end of a converged criteria rate is reached to investigate its capabilities following finishing the CSCSO stages. Complete the CSCSO stage to maximize the solutions make use of the area of search and the potential regions that the CSCSO discovered, and modify the Sailfish optimization algorithm. Assess the existing solution's fitness. Select a suitable group of the best-performing sand cats to serve as SFO's starting community. Use the chosen most effective approaches to start the sailfish and sardine populations. The initial positions of sailfish, as well as sardine fish, are denoted by Sio and Sdio accordingly.

3.3.3.4. Exploitation phase: SFO

Update Positions of Sailfish and Sardines:
After the iteration begins, update the newly current position of the sailfish and sardines respectively as per the equation stated above. Evaluate the fitness of the currently updated position of the sardine and sailfish respectively. Determine the best solution among the range of search areas that can be formulated as

$$P_{Slf\_best}^{t+1} = \underset{i}{argmax}\, Fitness\, P_{Slf\_new}^{t+1} \quad (26)$$

Update the best output solution ($P_{Slf\_best}^{t+1}$) from the set of possible ranges acquired after the convergent criteria of the iteration meet up, ending the optimization process. Finally, we acquired the non-redundant features which makes the classification as are more accurate and appropriate.

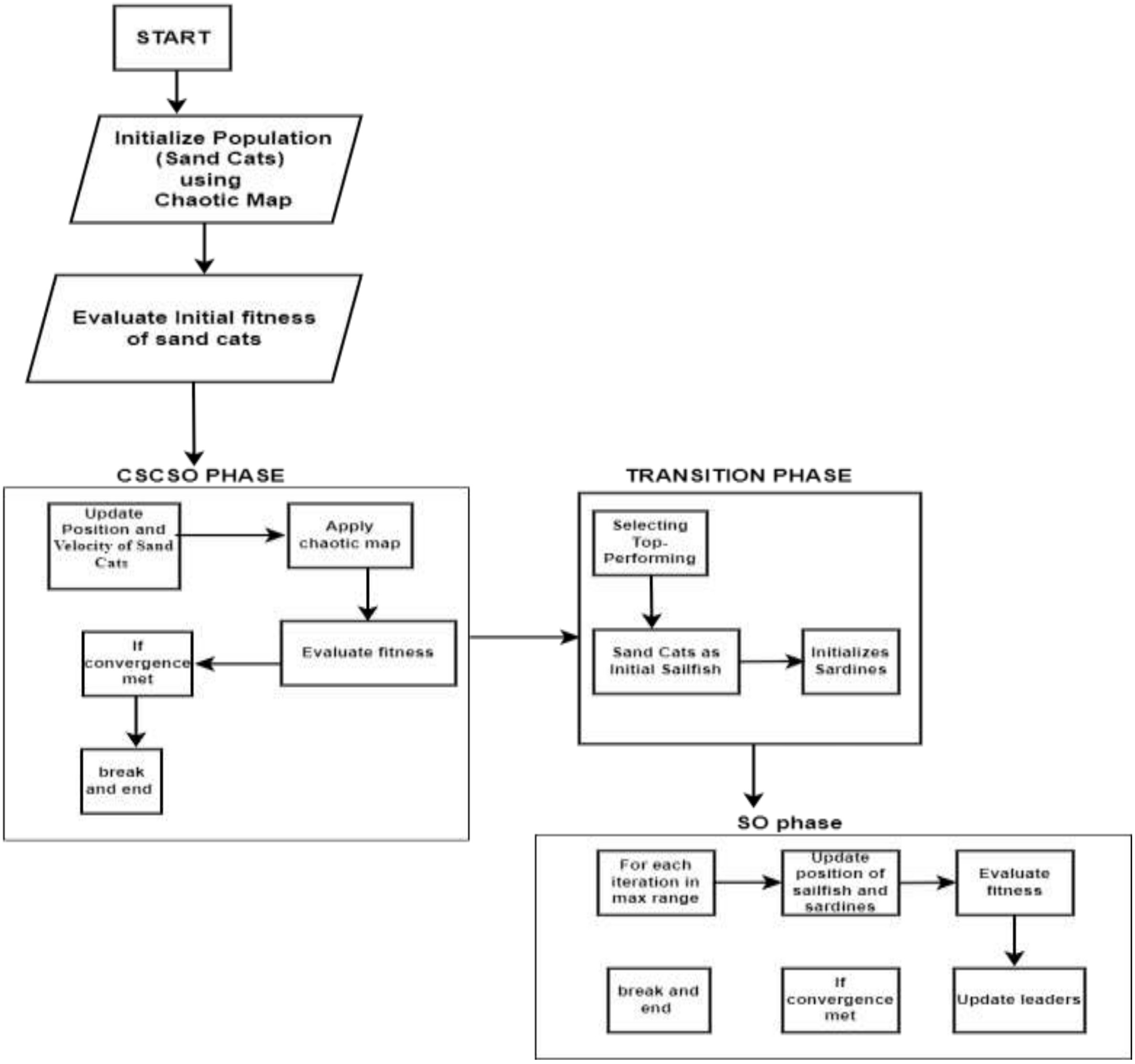

3.4. Classification
The non-redundant features obtained through the proposed model of the study are subjected to the classifier of ITAN. For time-sequenced-based series models of Encoder–decoder have been widely employed during the current era.

3.4.1. ITA Net
The model accepts three different types of covariates as inputs: covariates that are with class unknown (Q) that are represented as (xq); Time domain features of RR interval, PR Intervals, QRS Duration, P wave, and QT interval are mentioned as (xtd), other classes, such as supraventricular ectopic, Ventricular ectopic, non-ectopic, and the class of fusion that possesses both normal as well as ectopic features, are taken as the covariate of (xfe). The initial input lengths of xfeand xq are τlag,τlag+seq, τlag respectively by assuming a τseq-a horizon that defines the issue in question.

3.4.2. Input transformation layer
Since every covariate is a category variable, convert each categorical variable to a dic−d representations vector using label encoding along with the linear transformation. In this case, an empirical rule determines the length dimension dic:

$$d_i^c = \min\left(round\left(1.2 * (p_i^c)^{0.56}\right), \tilde{d}_i^c\right) \quad (27)$$

The rounding (•) function produces an appropriately rounded integer quantity, where pic and dic are the number of categories and the prescribed maximum encapsulation length for the ith. By trying to reduce error, the 1.2 and 0.56 in Eq. (2) practically give excellent confinement sizes for variables with subcategories.

3.4.3. Temporal covariate interpreter (TCI)

Due to the network's intricacy and expression capacity, TCI comprises an activation function of a softmax activation and a 2-layer forward feedback network. The modified representation of the ith covariate, covariate-wise significance matrix at time step t

Ctd ∈RM is created as follows, with tdm∈ℝ tdindicating it.

$$\mathbf{C_{td}} = \mathbf{ELU}\ (\mathbf{td^F W_1} + \mathbf{b_1})\ \mathbf{W_2} + \mathbf{b_2}, \quad (28)$$

$$\mathbf{td^f} = \mathbf{Flatten}\left(\left[\left(\mathbf{td_t^1}\right)^{\mathbf{T}}, \dots, (\mathbf{td_t^n})^{\mathbf{T}} \dots, (\mathbf{td_t^M})^{\mathbf{T}}\right]\right) \quad (29)$$

Where W1, W2, and b1, b2 are the accessible biases and weights of both the initial and second-line layers, respectively, and ELU is the Activation function of the Exponential Linear Unit. The Flatten (•) function creates a flattening vector across all covariates, where M is the total amount of covariates. The output of the TCI level StTCIat time step t can be written as follows after getting the covariate-wise significance vector:

$$\mathbf{S_t^{TCI}} = \sum_{\mathbf{n=1}}^{\mathbf{M}} \mathbf{C_{td}^{(n)}} \mathbf{td_t^n} \quad (30)$$

Where Ctd(n)is the nth element of Ctd.

3.4.4. LSTM layer

To extract time-related data, we process the input representation using an LSTM layer. The disregard, input, and output gates that make up an LSTM device regulate the transmission of two different types of information: the state that is hidden and the cell condition. The multi-head self-attention layer receives all-time stages from the LSTM algorithm layer and additional positioning information for attention modules from the concealed states. To avoid the need for extra positional encoders for the encoder as well as the decoder's inputs.

3.4.5. Multi-head attention layers

The focus mechanism records the long-range dependencies among the inputs. The Query, Key, which is and Values matrices' fundamental elements, Q, K, and V, stand for the following when computing the dot-product attention:

$$\mathrm{Attention}(\mathbf{Q}, \mathbf{K}, \mathbf{V}) = \mathrm{softmax}\left(\frac{\mathbf{QK^T}}{\sqrt{\mathrm{d_k}}}\right)\mathbf{V} \quad (31)$$

Where dk is the dimension of input, Multi-head attention, as an extension of the scaled dot-product attention, is more effective and is employed in our model:

$$\mathrm{MultiHead}(\mathbf{Q}, \mathbf{K}, \mathbf{V}) = \mathrm{Concat}(\mathrm{Head_1}, \dots, \mathrm{Head_H})\mathbf{W^0} \quad (32)$$

$$\mathrm{Head_i} = \mathrm{Attention}(\mathbf{QW_i^Q}, \mathbf{KW_i^K}, \mathbf{VW_i^V}) \quad (33)$$

WhereQWiQ,KWiK,VWiV, as well as W0 are learnable weights that conduct linear transformations and H is the number of attention heads.

3.4.6. Encoder–decoder architecture

In the era of RNN, encoder-decoder designs have been used to handle sequence input; this evolved recently with the invention of the mechanism for attention. To perform single-step inference, we use generative reasoning. In one decoding phase, the decoder receives the historical τseq-step value targets and produces the τseq-step predicting outcomes.

In summary, the determining forecasting results of y are generated as follows:

$$\hat{y}_{t:t+\tau_{seq}} = Dec\left(\left[X_{t:t+\tau_{seq}}^{fe}, \hat{X}_{t:t+\tau_{seq}}^{q}, y_{t-\tau_{seq}:t}\right], G_{t-\tau_{lag}}\right) \quad (34)$$

$$G_{t-\tau_{lag}} = Enc([X_{t-\tau_{lag}:t}^{td}, X_{t-\tau_{lag}:t}^{fe}, X_{t-\tau_{lag}:t}^{q}] \quad (35)$$

3.4.7. Covariate forecasting network

To possibly enhance predicting performance, we have added covariates from additional classes, such as Supraventricular ectopic, Ventricular ectopic, Non-ectopic, and Fusion of both normal and ectopic, which are included as a covariate of (xfe) into the decoder side inputs. The classes' variables are constrained, though. As a result, we provide a few crucial and predictable covariates from the combination class (xq) as input to the decoder side, which can also help the model operate better. To accomplish so, we recommend employing the covariate forecasting network to provide the class of fusing on the decoder side for certain time domain features:

$$\hat{x}_{t:t+\tau_{seq}}^{q} = CFN(x_{t-\tau_{lag}:t}^{q}) \quad (36)$$

At the final stage, all the redundant features are classified into five classes' supraventricular ectopic (S), non-ectopic (N), fusion (F), ventricular ectopic (V), and unknown (Q).

4. RESULTS AND DISCUSSION

A total of 25 records were taken from identical sets and allocated a sampling rate among 360 Hz, with 80% designated to be used for training as well as 20% for testing. Among these records, 23 were selected at random. The classification system is assessed using a test database at the recognition stage after it was successfully trained with previously acquired information or an enlisted data set [24]. We used a batch size of 25 and carried out fifty simulations in total for this paper. To prevent train and test information overlap, various patients with multisession ECG recordings were utilized.

4.1. Experimental setup

A computer equipped with an Intel i5-7300HQ processor, 16GB of RAM, and a GTX1050 GPU is used to train the proposed hybrid optimizer. The initial training process takes around 4236 seconds, while the ten-fold cross-verification procedure takes about 11 hours. An individual sample's median classification time is 0.198 milliseconds [25]. The programming language Python DL Toolbox is utilized in the algorithm's development.

4.2. Evaluation metrics

We use three metrics—accuracy (AC), recall, specificity (SPE), and precision (PR) based on true positive (TP), true negative (TN), false positive (FP), and false negative (FN) to assess the effectiveness of the Proposed model for arrhythmias categorization. The performance evaluation is provided in Equation (37–41).

4.2.1. Accuracy (ACC)

The proportion of accurate predictions to all predictions given in Eq. (37), or accuracy (ACC), is calculated. Determining whether the expenses of FP, as well as FN, are comparable is a better task for projecting the efficiency of the model.

$$ACC = \frac{T_p + T_n}{T_p + T_n + F_p + F_n} \tag{37}$$

4.2.2. Recall

Recall, as expressed in Eq. (38), is the proportion of TP to actual positives in the information, demonstrating the right categorization based on what occurred.

$$Recall = \frac{T_p}{T_p + F_n} \tag{38}$$

4.2.3. Precision (PR)

The ratio of expected TP for all the predicted positives, as shown in Eq. (39), is known as precision (PR).

$$PR = \frac{T_p}{T_p + F_p} \tag{39}$$

4.2.4. Specificity:

The percentage of TN that the algorithm accurately identified is known as specificity. It is also known as sensitivity. It assesses the capability of the model to recognize negative examples.

$$\text{Specificity} = \frac{TN}{TN + FP} \tag{40}$$

4.2.5. F1-score

The F1 value calculates how similar two items are to one another. It specifies the proportion between the combined size of the two entities and the amount of overlap size of its dual-segmented parts. The calculation for it is as follows:

$$\text{F1 Score} = \frac{2TP}{2TP + FP + FN} \tag{41}$$

4.2.6. ROC Curve:

The compromise between the two parameters of sensitivity as well as specificity is graphically represented by the ROC curve, where the TP rate is represented by the y-axis and the rate of FP is represented by the x-axis. The TP rate and FP rate are used to plot the ROC curve, which visually depicts the general efficacy of the proposed model.

The compromise between both specificity and sensitivity is graphically represented by the ROC curve where the rate of TP results is represented on the vertical axis and the rate of FP is represented on the horizontal axis of the graph. The TPR as well as FPR are used to generate the ROC curve, which illustrates the overall efficacy of the proposed model.

A series of research was carried out to evaluate the performance of the suggested strategy's steps to demonstrate the approach's efficacy. In the first experiment, FIR and IIR noise reduction techniques were used to deduce the noise from

the ECG signal. To pick attributes from the pre-processed data, the hybrid model based on the CSCSO and SO algorithm was utilized. The non-redundant features are finally classified with the classifier of Interpretable Temporal Attention network into the five different classes including supraventricular ectopic (S), non-ectopic (N), fusion (F), ventricular ectopic (V), and unknown (Q).
The unprocessed ECG signal extracted from the database of MIT-BIH arrhythmia illustrated in Figure 3 has deviated due to a lot of interruptions taking place during the recording session due to its low amplitude nature. This can lead to an increase in the misclassification rate. So we subject the raw signal to the filter of infinite impulsive response as well as finite impulsive response.

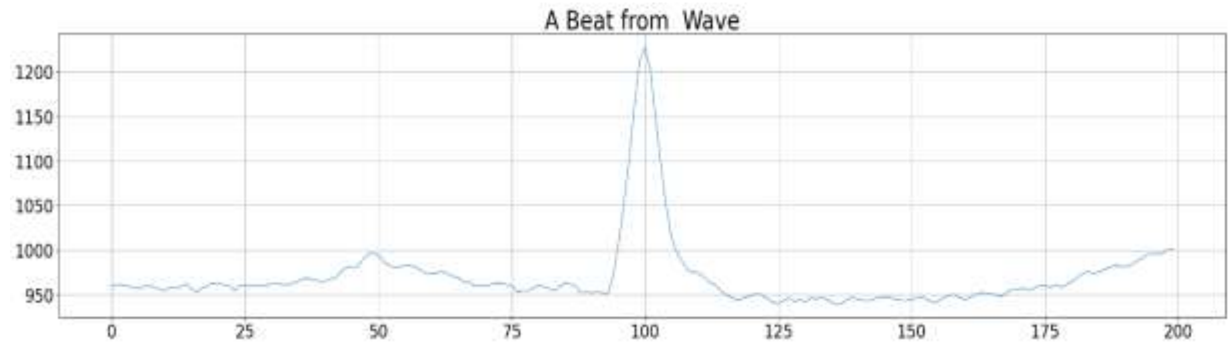

Figure 3 illustrates the beat from the ECG wave.

When the FIR filter is applied to the noisy ECG signal. It is well known that for transmission and filtering to be distortionless, the system's amplitude response must remain constant within the signal's effective spectral range and its phase response must follow a linear relationship with frequency, or linear phase. The FIR filter can accomplish linear phase filtering, compared to the IIR filter. Furthermore, because the FIR filter is an all-zero filter, both its software and hardware architectures can be designed without taking the problem of stability into account. FIR filters have consequently been used extensively for signal noise reduction.

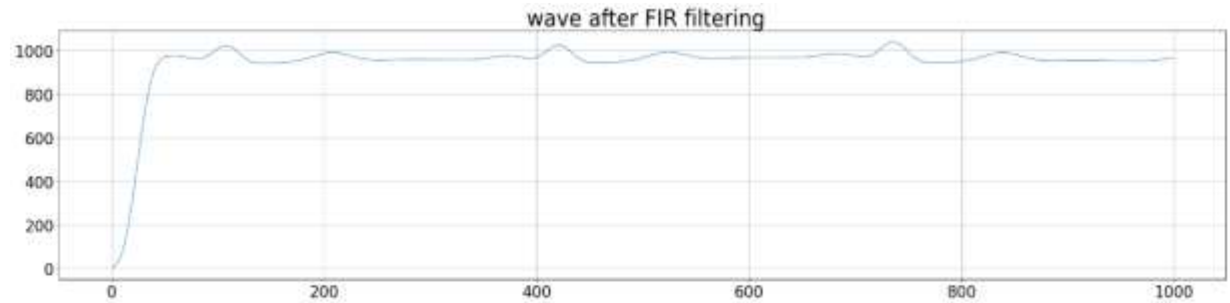

Figure 4. Illustrates the pre-processed wave by FIR Filter.

The ECG signal was applied to the IIR filter to eliminate noise from ECG signals. Advantages of an IIR filter the signal passing through the filter is not distorted.

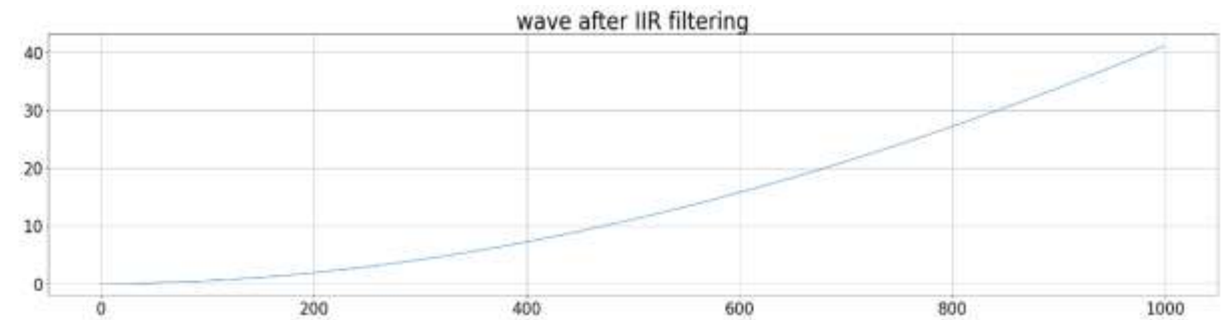

Figure 5. Illustrates the pre-processed wave by FIR Filter.

We proposed using a hybrid model of an SO along with a CSCSO algorithm for the proceedings of feature selection. By redundant attributes that constitute the signal that drives the process of classification to be extremely accurate, the approach to selecting features aims to improve the databases. Due to the chaos criterion thrown onto them, the CSCSO Algorithm is known to have a benefit in the range of exploration. Additionally, sailfish optimization employs hunting techniques using sardines that are enhanced with exploratory traits. We suggested a hybrid model that would make use of each of the optimization techniques' potential and the benefit of exploration. Performance metric values of the overall methodology are compared below as they are illustrated in Table 2 with the feature selection and without feature selection.

Table 2. Depicts the Performance metrics

PERFORMANCE METRICS	WITHOUT FEATURE SELECTION	WITH CSCSO OPTIMIZER	WITH SO OPTIMIZER	HYBRID MODEL CSCSO-SO
ACCURACY	95.3%	97.8%	97.5%	99.95%
PRECISION	91.2%	95.2%	93.1%	99.4%
RECALL	86.8%	91.2%	95.4%	99.19%
F1-SCORE	87.4 %	96.52%	97.25%	98.76%
SPECIFICITY	91.4%	92.42%	95.4%	99.21%

The classifier of the interpretable temporal attention network of the encoder-decoder structure is applied to the independent signals. This classifier separates every component of the time domain feature, all classes, and unknowns into distinct covariates. It is used together with the input transformation layer to ensure that the TCI determines the significance of each covariate by inducing characteristics with high dimensions. Then, an LSTM layer for temporal attribute extraction and a multi-head self-attention layer for long-range dependence acquisition is connected to both the decoder and encoder sides of the TCI layer. The decoder consists of three additional components: a covariate forecasting network (CFN) for expanding differentiated classes, a layer of linearity for the final stage of the regression model, and an encoder-decoder attention layer for monitoring the encoding process participation. Lastly, it groups the datasets into the following classes: unknown (Q), fusion (F), ventricular ectopic (V), supraventricular ectopic (S), and non-ectopic (N).

In this case, the x-axis indicates the overall quantity of model development epochs, or training cycles, throughout the entire dataset, while the y-axis displays the accuracy and loss, appropriately. As the quantity of epochs increases, both the accuracy of the validation and training curves trend progressively. As the figure below illustrates, there is an upsurge in both the level of accuracy as well as the amount of misperception.

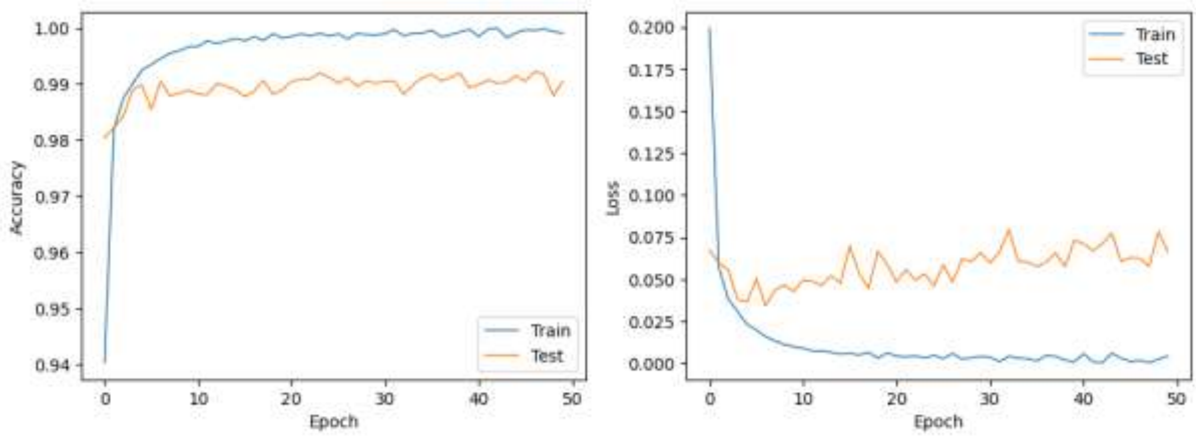

Figure 6 shows the Accuracy-loss curve.

The remaining amount classes of heartbeat datasets are ignored in other classes since the vast majority of Normal heartbeats in the MIT-BIH AD (around 80%) are standard (N). Consequently, 82,994 heartbeat segments were included in this analysis: 7129 as supraventricular ectopic (S), 75028 are classified as normal (N), 33 as fusion (F), 802 as ventricular ectopic (V), and 2 as unknown (Q). The graph below was used to assess the performance of the algorithm available in the datasets used for training and testing, exhibiting their precision, recall, and F1-score metrics. The recall, precision, and F1-scores of the classes of supraventricular ectopic (S), Normal (N), Fusion (F), ventricular ectopic (V), and unknown (Q), as well as 99.4, 99.6, 99.6, 99.3, and 99.5, are increased.

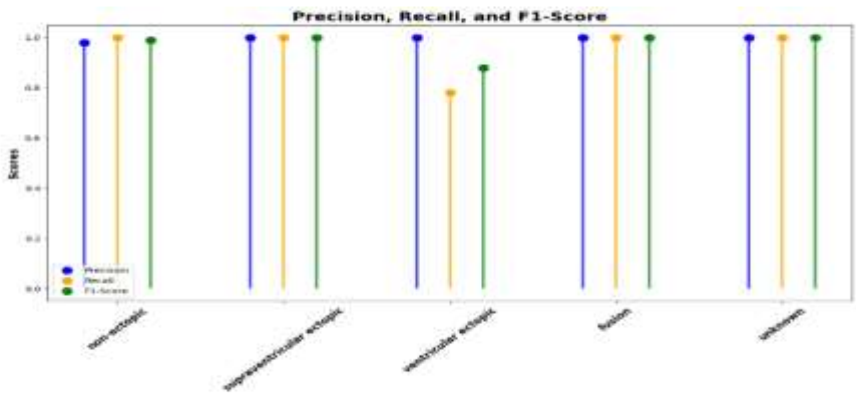

Figure 7. Illustrates the Precision, recall, and F1-score

The expected vs. reality results for classification are presented in the confusion matrix table. The output of positive versus negative outcomes of tests is described in the matrix of confusion table. The results of the classification of the proposed hybrid CSCSO-SO model are displayed in the confusion matrix. All five classes of heartbeats have an overall classification accuracy rate of 99.98, 99.97, 99.92, 99.3, and 99.2, which demonstrates the efficacy of the model.

An additional measuring score for assessing the extent to which the model discriminates between classes is called ROC. It calculates the compromise between true-positive as well as false-positive rates, which a ROC curve can be used to graphically depict. The ROC curve is displayed in Figure 9. Except for class 0 (0.98 percent), every study class is depicted in the figure as having a perfect score.

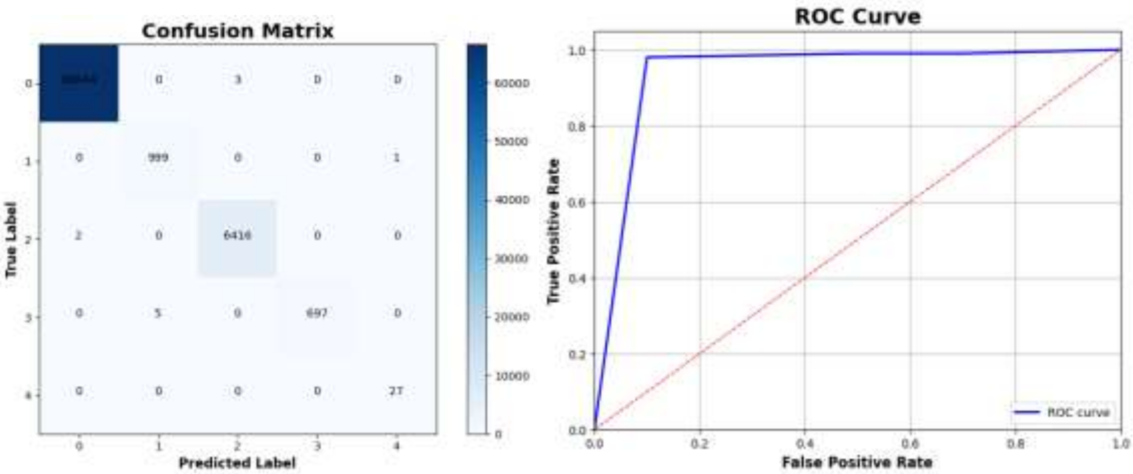

Figures 8 and 9. Illustrates the confusion matrix and ROC Curve.

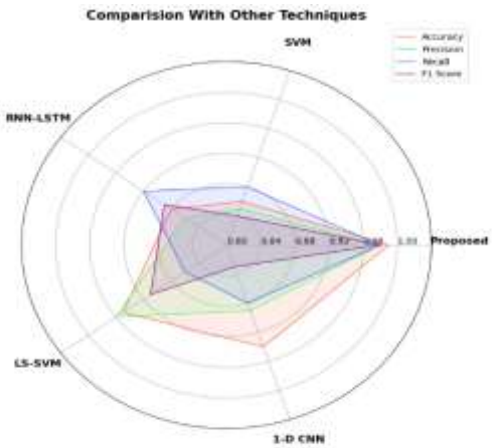

Figure 10. Illustrates the comparison of classifier

The existing research on ECG classification is depicted in the figure. Although the sets of data utilized in this literature diverge, the comparison is still valuable. Using 1D-CNN, the five primary classes were recognized with an accuracy rate of 94.61%. An SVM classifier on heartbeat classifications achieved 98.18% accuracy. In their research, RNN-LSTM performed 94.52% on the five classes of N, Q, S, V, and F. Long-duration ECG signals were categorized using LS-SVM, which produced 94.6% accuracy on arrhythmias classifications in the MIT-BIH database. The model we propose outperforms the other existing models and delivers an accuracy of 99.95% when compared with other models.
A wide range of methods for choosing features has also been used to evaluate the proposed approach of CSCSO-SO including the MPMO algorithm, whale optimization WOA-PNN, flamingo-optimization (FO), and Algorithm of (SO-SOARO). The results of the comparison of CSCSO-SO with MPMO, WOA, FO, and SO-SOARO are displayed in the table. While the WOA gained 99.43%, the MPMO achieved 99.95%, and the FO achieved 97-88%, the accuracy of SO-SOARO accumulated at 98.89%

Table 3. Depicts the comparative performance

EXISTING METHOD	FEATURES APPROACHES	ACCURACY %
Nijaguna et al.[26]	SO-SOARO	98.89
Qaisar et al. [27]	MPMO	98.95
Li et al. [28]	WOA	99.43
Kumar et al [29]	FO	97.88
PROPOSED	CSCSO-SO	99.95

The investigation reveals that our suggested model outperforms the current techniques in terms of performance.

5. CONCLUSION

The ECG is a portable instrument that records cardiac signals for use in emergencies. However, its suitable interpretation has been complicated by its complexities and transmitted noise. The ECG signal's low magnitude, and complexity as well. Non-linearity makes it challenging to classify data quickly and accurately by hand. Because of that, a computerized procedure that can distinguish irregular heartbeats from data from ECG should be created for utilization by the medical industry. We presented a hybrid model of the SO as well as the CSCSO in this article. To assess the outcomes, a matrix of confusion and other performance indicators, including ROC, recall, sensitivity, specificity, as well as precision, were provided. The proposed approach has effectively classified arrhythmia into the following groups: supraventricular ectopic (S), non-ectopic (N), fusion (F), ventricular ectopic (V), and unknown (Q) when compared with the most sophisticated methods. As a result, the proposed strategy may be employed as a supplementary tool to help physicians diagnose arrhythmias. One of the most important tasks we had to complete for this research was data augmentation. The quantity of data utilized will be raised in subsequent studies. Additionally, the impact of this circumstance will be investigated on the optimizing hybrid model that has been proposed.

REFERENCES

1. Sangaiah, A. K., Arumugam, M., & Bian, G. B. (2020). An intelligent learning approach for improving ECG signal classification and arrhythmia analysis. Artificial intelligence in medicine, 103, 101788.
2. Kuila, S., Dhanda, N., & Joardar, S. (2022). ECG signal classification and arrhythmia detection using ELM-RNN. Multimedia Tools and Applications, 81(18), 25233-25249.
3. Atal, D. K., & Singh, M. (2020). Arrhythmia classification with ECG signals based on the optimization-enabled deep convolutional neural network. Computer Methods and Programs in Biomedicine, 196, 105607.
4. Mathunjwa, B. M., Lin, Y. T., Lin, C. H., Abbod, M. F., & Shieh, J. S. (2021). ECG arrhythmia classification by using a recurrence plot and convolutional neural network. Biomedical Signal Processing and Control, 64, 102262.
5. Arumugam, M., & Sangaiah, A. K. (2020). Arrhythmia identification and classification using wavelet centered methodology in ECG signals. Concurrency and computation: practice and experience, 32(17), e5553.
6. Zhang, S., Lian, C., Xu, B., Su, Y., & Alhudhaif, A. (2024). 12-Lead ECG signal classification for detecting ECG arrhythmia via an information bottleneck-based multi-scale network. Information Sciences, 662, 120239.
7. Dias, F. M., Monteiro, H. L., Cabral, T. W., Naji, R., Kuehni, M., & Luz, E. J. D. S. (2021). Arrhythmia classification from single-lead ECG signals using the inter-patient paradigm. Computer Methods and Programs in Biomedicine, 202, 105948.
8. Kuila, S., Dhanda, N., & Joardar, S. (2023). ECG signal classification to detect heart arrhythmia using ELM and CNN. Multimedia Tools and Applications, 82(19), 29857-29881.
9. Che, C., Zhang, P., Zhu, M., Qu, Y., & Jin, B. (2021). Constrained transformer network for ECG signal processing and arrhythmia classification. BMC Medical Informatics and Decision Making, 21(1), 184.
10. Ullah, A., Rehman, S. U., Tu, S., Mehmood, R. M., Fawad, & Ehatisham-ul-Haq, M. (2021). A hybrid deep CNN model for abnormal arrhythmia detection based on cardiac ECG signal. Sensors, 21(3), 951.
11. Sharma, P., Dinkar, S. K., & Gupta, D. V. (2021). A novel hybrid deep learning method with cuckoo search algorithm for classification of arrhythmia disease using ECG signals. Neural Computing and Applications, 33(19), 13123-13143.
12. Çınar, A., & Tuncer, S. A. (2021). Classification of normal sinus rhythm, abnormal arrhythmia and congestive heart failure ECG signals using LSTM and hybrid CNN-SVM deep neural networks. Computer methods in biomechanics and biomedical engineering, 24(2), 203-214.
13. Rahman, A. U., Asif, R. N., Sultan, K., Alsaif, S. A., Abbas, S., Khan, M. A., & Mosavi, A. (2022). ECG classification for detecting ECG arrhythmia empowered with deep learning approaches. Computational intelligence and neuroscience, 2022(1), 6852845.
14. Abdalla, F. Y., Wu, L., Ullah, H., Ren, G., Noor, A., Mkindu, H., & Zhao, Y. (2020). Deep convolutional neural network application to classify the ECG arrhythmia. Signal, Image and Video Processing, 14, 1431-1439.
15. Ahmed, A. A., Ali, W., Abdullah, T. A., & Malebary, S. J. (2023). Classifying cardiac arrhythmia from ECG signal using 1D CNN deep learning model. Mathematics, 11(3), 562.
16. Sharma, P., & Dinkar, S. K. (2022). A linearly adaptive Sine–cosine algorithm with application in deep neural network for feature optimization in arrhythmia classification using ECG signals. Knowledge-based systems, 242, 108411.
17. Ullah, A., Anwar, S. M., Bilal, M., & Mehmood, R. M. (2020). Classification of arrhythmia by using deep learning with 2-D ECG spectral image representation. Remote Sensing, 12(10), 1685.
18. Wu, M., Lu, Y., Yang, W., & Wong, S. Y. (2020). A study on arrhythmia via ECG signal classification using the convolutional neural network. Front Comput Neurosci 14.
19. Bhatia, S., Pandey, S. K., Kumar, A., & Alshuhail, A. (2022). Classification of electrocardiogram signals based on hybrid deep learning models. Sustainability, 14(24), 16572.
20. Madan, P., Singh, V., Singh, D. P., Diwakar, M., Pant, B., & Kishor, A. (2022). A hybrid deep learning approach for ECG-based arrhythmia classification. Bioengineering, 9(4), 152.
21. Sowmya, S., & Jose, D. (2022). Contemplate on ECG signals and classification of arrhythmia signals using CNN-LSTM deep learning model. Measurement: Sensors, 24, 100558.

22. Ganguly, B., Ghosal, A., Das, A., Das, D., Chatterjee, D., & Rakshit, D. (2020). Automated detection and classification of arrhythmia from ECG signals using feature-induced long short-term memory network. IEEE Sensors Letters, 4(8), 1-4.
23. Mian Qaisar, S., & Hussain, S. F. (2023). An effective arrhythmia classification via ECG signal subsampling and mutual information based subbands statistical features selection. Journal of Ambient Intelligence and Humanized Computing, 14(3), 1473-1487.
24. Pandey, S. K., Shukla, A., Bhatia, S., Gadekallu, T. R., Kumar, A., Mashat, A., ... & Janghel, R. R. (2023). Detection of arrhythmia heartbeats from ECG signal using wavelet transform-based CNN model. International Journal of Computational Intelligence Systems, 16(1), 80.
25. Sanamdikar, S. T., Hamde, S. T., & Asutkar, V. G. (2020). Analysis and classification of cardiac arrhythmia based on general sparsed neural network of ECG signals. SN Applied Sciences, 2(7), 1244.
26. Nijaguna, G. S., Lal, N. D., Divakarachari, P. B., De Prado, R. P., Woźniak, M., & Patra, R. K. (2023). Feature selection using selective opposition based artificial rabbits optimization for arrhythmia classification on Internet of medical things environment. IEEE Access.
27. Qaisar, S. M., Khan, S. I., Srinivasan, K., & Krichen, M. (2023). Arrhythmia classification using multirate processing metaheuristic optimization and variational mode decomposition. Journal of King Saud University-Computer and Information Sciences, 35(1), 26-37.
28. Li, N., He, F., Ma, W., Wang, R., Jiang, L., & Zhang, X. (2022). The identification of ecg signals using wavelet transform and woa-pnn. Sensors, 22(12), 4343.
29. Kumar, A., Kumar, M., Mahapatra, R. P., Bhattacharya, P., Le, T. T. H., Verma, S., ... & Mohiuddin, K. (2023). Flamingo-optimization-based deep convolutional neural network for IoT-based arrhythmia classification. Sensors, 23(9), 4353.